

Time-resolved infrared spectroscopy of nematic-liquid-crystal electro-optic switching

Won Gun Jang and Noel A. Clark

Ferroelectric Liquid Crystal Materials Research Center, Department of Physics, University of Colorado, Boulder, Colorado 80309-0390

(Received 18 July 2000; published 27 February 2001)

Time resolved infrared (IR) vibrational absorption spectroscopy is used to probe the dynamics of electric field-induced reorientation of the biphenyl molecular core and alkyl tail subfragments of the nematic liquid crystal 5CB (4-pentyl-4'-cyanobiphenyl). The planar to homeotropic transition, induced by application of an electric field step to high pre-tilt planar aligned cells, is studied for switching times ranging from 200 μ s down to 8 μ s, the latter a factor of 1000 times faster than any previous nematic IR study. The reorientation rates of the core and tail are found to be the same to within experimental uncertainty, and scale inversely with applied field squared, as expected for the balance of field and viscous torques. Thus any molecular conformation change during switching must relax on a shorter time scale. A simple model shows that these data eliminate the possibility of there being substantial differences between the reorientational dynamics of the tails and cores on the time scales longer than on the order of 10 μ s.

DOI: 10.1103/PhysRevE.63.031707

PACS number(s): 61.30.Gd, 78.30.Jw

I. INTRODUCTION

The rod-shaped molecules which form liquid crystals (LCs) typically have a rigid central core (to provide the steric interaction of rigid rods that stabilizes orientationally ordered phases) and flexible tails (to suppress crystallization). In electro-optic applications the LC mean molecular long axis, given by the director field $\mathbf{n}(\mathbf{r})$, reorients in applied field with an overdamped response limited by orientational viscosity. Molecular optical anisotropy is then exploited to achieve an electro-optic effect. An important aspect of such electro-optic behavior of LCs is the *intramolecular* dynamics probed by the measurement of the reorientation response of different molecular subfragments during switching. Such studies provide information on molecular conformation change during driven collective reorientation, which can be correlated with the distribution of field-induced torques and intermolecular forces applied to the molecule. In this paper we study, using time-resolved Fourier transform infrared (FTIR) spectroscopy, the field-driven reorientation of the core and tail groups of the nematic liquid crystal 4-pentyl-4'-cyanobiphenyl (5CB), shown in Fig. 1, during electro-optic switching of $\mathbf{n}(\mathbf{r})$.

In recent years, FTIR and Raman spectroscopy have proven to be powerful probes of the molecular conformation and orientation in LC phases [1], and both have been applied in dynamical studies. Vibrational spectroscopy selects molecular vibrational modes, each of which has a transition dipole and polarizability tensor, fixed relative to the molecule or a molecular subfragment, which couples the vibration to incident IR or visible light, respectively. Measurement of IR absorbance or Raman intensity vs polarization orientation relative to the symmetry axes of a macroscopically single domain sample then enables the moments of the transition dipole or polarizability tensor, and, therefore, moments of the molecular orientation distribution to be determined. Improvement in electronics and data acquisition processes have enabled time resolved vibrational spectroscopy with time resolution approaching a few nanoseconds [2].

To date, although there have been a number of studies of

intramolecular LC dynamics utilizing vibrational spectroscopy, mostly focusing on the relative motion of core and tail, no coherent picture of intramolecular motion has emerged. Some have reported no considerable differences in reorientation rates of the mesogenic core and tails [3–6]. In other reports, the motion of the flexible tail part *precedes* that of the core [7,8], and in still others, the motion of the core precedes that of the flexible part [9–14].

This report analyzes the switching dynamics of a planar-

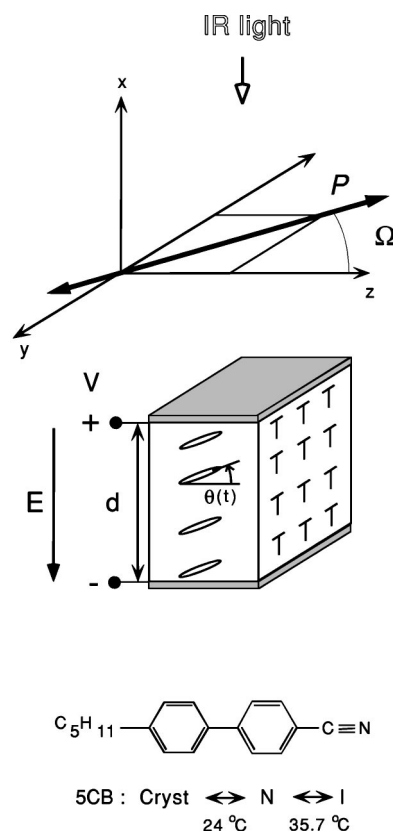


FIG. 1. Schematic diagram of the experimental geometry, the liquid crystal 5CB (4-pentyl-4'-cyanobiphenyl), and its phase diagram.

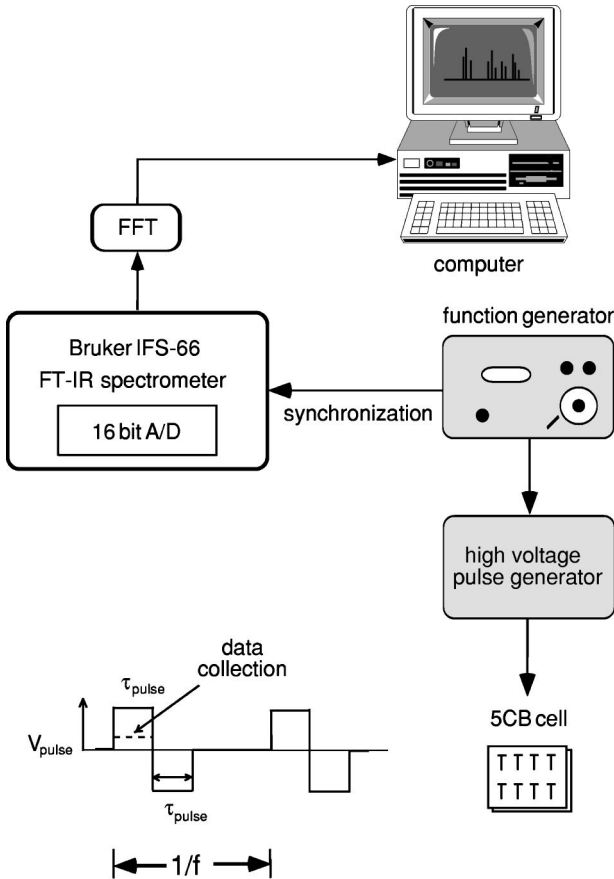


FIG. 2. Schematic diagram of step-scan FTIR electronics, showing the bipolar pulse waveform driving the 5CB. Data collection is carried out during the positive part of the pulse of width τ_{pulse} . The negative part of the pulse provides dc balance.

aligned cell of high pre-tilt nematic liquid crystal 5CB by observing changes of absorbance due to vibrations of the biphenyl core, cyano group, and alkyl tail, as a function of time following application of the external electric field. 5CB has a large positive dielectric anisotropy, $\Delta\epsilon = \epsilon_{\parallel} - \epsilon_{\perp}$, arising almost entirely from the $\text{C}\equiv\text{N}$ dipole parallel to the core axis, so that the driving field acts on the core.

II. EXPERIMENTS

The overall experimental setup is illustrated in Fig. 2. FTIR time-resolved spectroscopy was carried out using a step-scan Bruker IFS 66 spectrometer, equipped with a photovoltaic mercury cadmium telluride detector, a 50 MHz pre-amplifier, and an internal ADC board to detect modulated IR signal. A periodic sequence of bipolar pulses, of amplitude V_{pulse} and width for each polarity interval τ_{pulse} ($50 < \tau_{\text{pulse}} < 1000 \mu\text{s}$), shown in Fig. 2, is applied to the liquid crystal cell using a function generator which can generate pulses with up to $\pm 1000 \text{ V}$ amplitude with $\sim 10 \text{ ns}$ risetime [15]. Bipolar pulses were employed in order to maintain dc balance on the liquid crystal and τ_{pulse} was decreased with increasing V_{pulse} such that the pulse ended soon after switching was completed, in order to reduce the occurrence of dielectric breakdown of the LC at high voltage. The pulse fre-

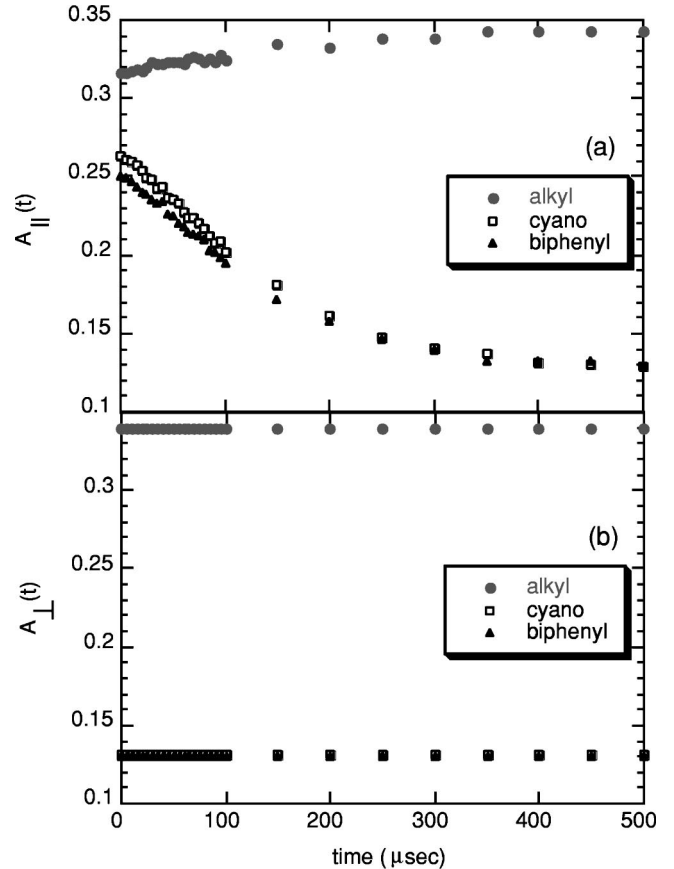


FIG. 3. Time variation of absorbance of the biphenyl, cyano, and alkyl modes as a function of time upon application of a 25 V for IR polarization parallel to ($A_{\parallel}(t)$) and normal to ($A_{\perp}(t)$) the \mathbf{x} - \mathbf{z} plane of rotation of \mathbf{n} . $A_{\perp}(t)$ is independent of t since the polarization is normal to \mathbf{n} throughout its reorientation. $A_{\parallel}(t) \rightarrow A_{\perp}(t)$ at large t .

quency selection of 1 KHz was based on the trade-off between maximizing the data collection rate (favoring a higher frequency) and allowing the director to relax between pulses (favoring a lower frequency). Synchronized TTL trigger pulse signals for data sampling are fed onto the 16-bit analog-to-digital converter of the main spectrometer. Spectrometer transmission is collected while both interferometer path difference and time delay following reversal of the voltage on the LC cell are evolving. Thirty independent measurements are made at each mirror position and time delay. The computer then sorts, averages, and Fourier transforms the data to obtain spectra vs time delay.

The experimental cell geometry is shown in Fig. 1. The 5CB was planar aligned in IR transparent capacitor made from CaF_2 windows coated with a 100 \AA thick layer of indium tin oxide for electrodes, and 200 \AA thick rubbed Nissan RN768 polyimide alignment layers. The plates were rubbed antiparallel and subjected to a 50 min soft-bake/2 hour hard-bake process [16] to produce a uniform $\mathbf{n}(\mathbf{r})$, in the \mathbf{x} - \mathbf{z} plane of the rubbing, pretilted by $\sim 13^\circ$ from the plane of the substrates. The spacing between the plate was $d \sim 6 \mu\text{m}$. The ITO electrode is $\cong 1 \text{ cm}^2$ in area, with sheet resistivity $R = 100 \Omega/\square$, giving the cell an intrinsic RC time

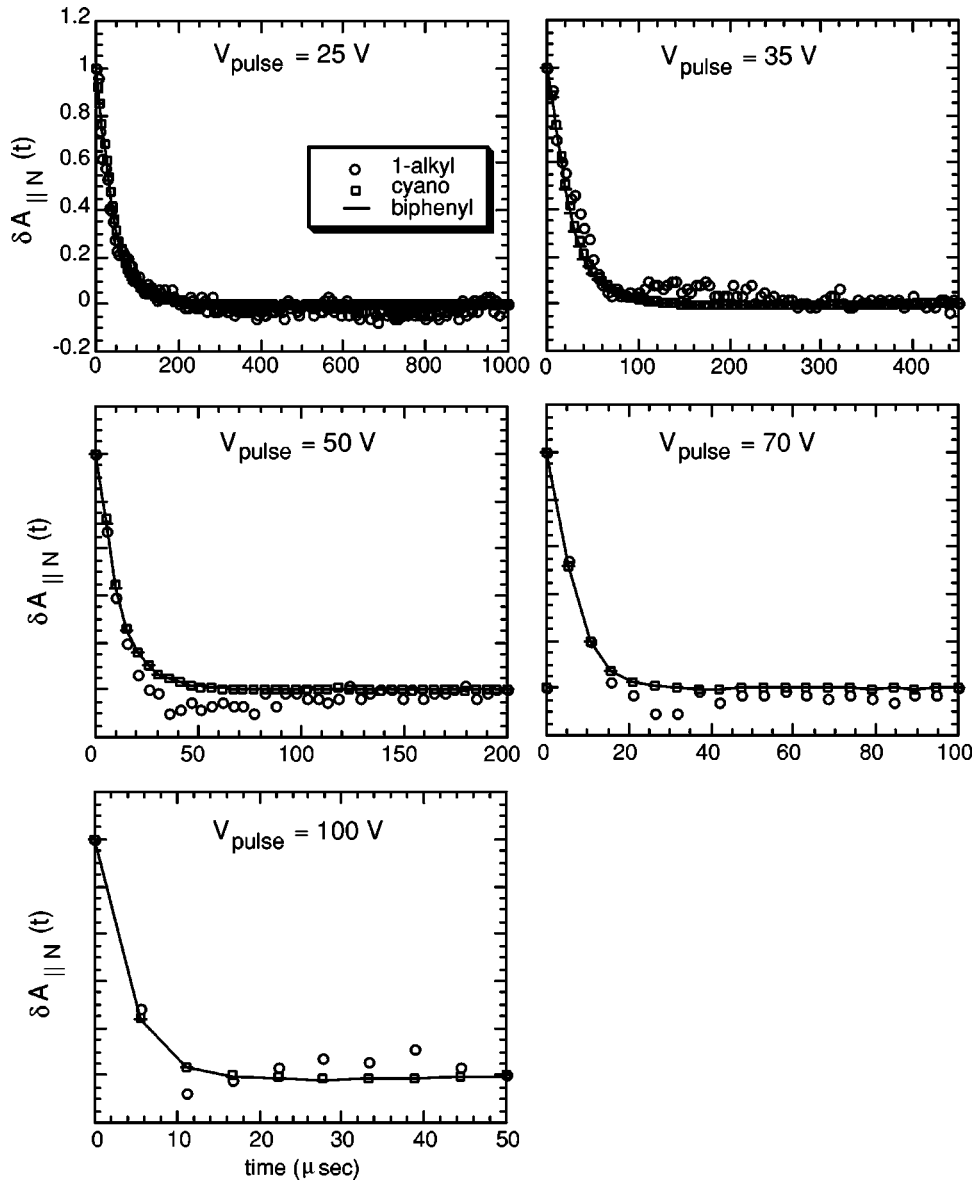


FIG. 4. Time dependence of the normalized absorbance for IR polarization parallel to the plane of reorientation of \mathbf{n} of the biphenyl, cyano, and alkyl modes upon application of pulses of indicated voltages. The overlap of biphenyl, cyano, and alkyl data shows that there is no systematic difference in the reorientation dynamics of the three molecular subunits on time scales longer than $5 \mu\text{s}$.

constant which determines the shortest time interval over which an applied voltage step appears on the liquid crystal. When filled with LC, this RC time is $\sim 2 \mu\text{s}$, which is the limiting time resolution of the experiment. This time is shorter than the fastest LC response time observed here ($\sim 8 \mu\text{s}$) and will be ignored.

IR light is incident normal to the cell plates and linearly polarized in the \mathbf{y} - \mathbf{z} plane at an angle Ω relative to the \mathbf{x} - \mathbf{z} plane. Raw spectra are then baseline corrected and values of absorbance peaks determined. Data are presented here for peaks at 2930 , 2227 , and 1606 cm^{-1} , due to the *alkyl* tail CH_2 stretching modes, *cyano* and *phenyl* core stretching modes, respectively.

The electrostatic torque due to the applied field $\mathbf{E} = E\mathbf{x}$ tends to rotate $\mathbf{n}(\mathbf{r})$ to be parallel to \mathbf{E} , normal to the plates. This induced reorientation, entirely in the \mathbf{x} - \mathbf{z} plane, is continuous because at $t=0$ $\mathbf{n}(\mathbf{r})$ is tilted from \mathbf{z} axis, through θ_0 , because of the partial relaxation of $\mathbf{n}(\mathbf{r})$ between pulses. Assuming normal incidence and $\mathbf{n}(\mathbf{r})$ to be in the \mathbf{x} - \mathbf{z} plane, the

two electromagnetic IR eigenmodes are linearly polarized along \mathbf{z} and \mathbf{y} , and the IR absorbance can be completely characterized by determination of A_{\parallel} , measured with $\Omega = 0^\circ$ (the IR light polarized parallel to the \mathbf{x} - \mathbf{z} plane), and A_{\perp} measured with $\Omega = 90^\circ$ (the IR light polarized perpendicular to the \mathbf{x} - \mathbf{z} plane). These polarizations are set using a wire-grid IR polarizer located between the IR source and sample. $A_{\parallel}(t)$ and $A_{\perp}(t)$ were recorded at $5 \mu\text{s}$ time intervals following voltage application at $t=0$.

III. MODELS

A basic goal of this kind of experiment is to probe changes in molecular conformation and/or distribution during field-induced reorientation. Obviously, the macroscopic symmetry axes, as characterized by eigenvectors of the optical dielectric or magnetic susceptibility tensors, reorient. In general, in addition to this reorientation the eigenvalues, e.g., the principle refractive indices, will be field dependent, as

will the distributions of molecular subfragments. We consider here a basic model of such reorientation using a generalized variable $\Psi(t)$ to characterize the extent to which the molecule is out of its equilibrium conformation distribution during switching. Thus, $\Psi(t)$ may represent the mean bend angle between the axes of the core and alkyl tail, or may represent some moment of the orientational distribution of a subfragment. Alternatively, during the field-induced reorientation of the mean molecular long axis in the \mathbf{x} - \mathbf{z} plane the nematic symmetry is biaxial, and $\Psi(t)$ could characterize the degree of biaxiality. The effective mechanical model determining the time dependence of $\Psi(t)$ is shown in Fig. 3. $\Psi(t)$ is the displacement of a damped harmonic oscillator driven through a dashpot. As is almost always the case for calculation of the viscous response of liquid crystals the mass term in the equation of motion is negligible after a very fast (ps) inertial relaxation and may be set to zero, leaving the equation of motion

$$-K\Psi(t) = D \frac{d}{dt} [\Psi(t) - \alpha\omega(t)]$$

or

$$-\Gamma\Psi(t) = \frac{d}{dt} [\Psi(t) - \alpha\omega(t)].$$

Here D is the dashpot dissipative coefficient, K is the effective force restoring the equilibrium state (at the relaxation rate $\Gamma = K/D$), α is a coupling coefficient, and $\omega(t)$ is the driven director angle of orientation, evolving from $\omega \sim 0$ to $\omega \sim \pi/2$ through the planar to homeotropic transition. For planar to homeotropic field-induced switching $d\omega(t)/dt$ is a peaked function of width comparable to the switching time t_R , of maximum value approximately equal to $\pi/2t_R$, and of time-integrated area $\sim \pi/2$. For slow switching ($\Gamma t_R > 1$), $d\Psi(t)/dt$ is negligible and $\Psi(t) = \Gamma^{-1} d/dt [\alpha\omega(t)]$, proportional to the reorientation rate, with a maximum value $\Psi_{\max} \sim \alpha\pi/2\Gamma t_R$. For fast switching ($\Gamma t_R < 1$), $\omega(t)$ can be approximated as a linear ramp from $\omega = 0$ at $t = 0$ to $\omega = \pi/2$ at $t = t_R$, during which $\Psi = \alpha\omega(t)$. At the termination of the switching $\Psi(t = t_R) = \Psi_{\max} = \alpha\omega/2$, exponentially decaying for $t > t_R$ with the rate Γ : $\Psi(t > t_R) = (\alpha\pi/2)\exp[-\Gamma(t - t_R)]$. This model shows that in order to observe dynamically induced conformation conditions the latter situation ($\Gamma t_R < 1$) is the most favorable, and would appear as a partial dichroism change over a time during switching depending on applied voltage, followed by a field-independent relaxation to complete the change.

In absence of such relaxational effects the reorientation response is limited by viscosity. In order to qualitatively compare the reorientational dynamics of the three modes, we calculate the normalized absorbance change $\delta A_{\parallel N}(t)$,

$$\delta A_{\parallel N}(t) = [A_{\parallel \text{sat}} - A_{\parallel}(t)] / [A_{\parallel \text{sat}} - A_{\parallel}(0)], \quad (1)$$

where $A_{\parallel}(t)$ is the absorbance measured with IR polarization in the \mathbf{x} - \mathbf{z} plane of rotation of $\mathbf{n}(\mathbf{r})$, and $A_{\parallel}(0)$ is the initial absorbance, determined by the $t = 0$ tilt of $\mathbf{n}(\mathbf{r})$, and $A_{\parallel \text{sat}}$ is

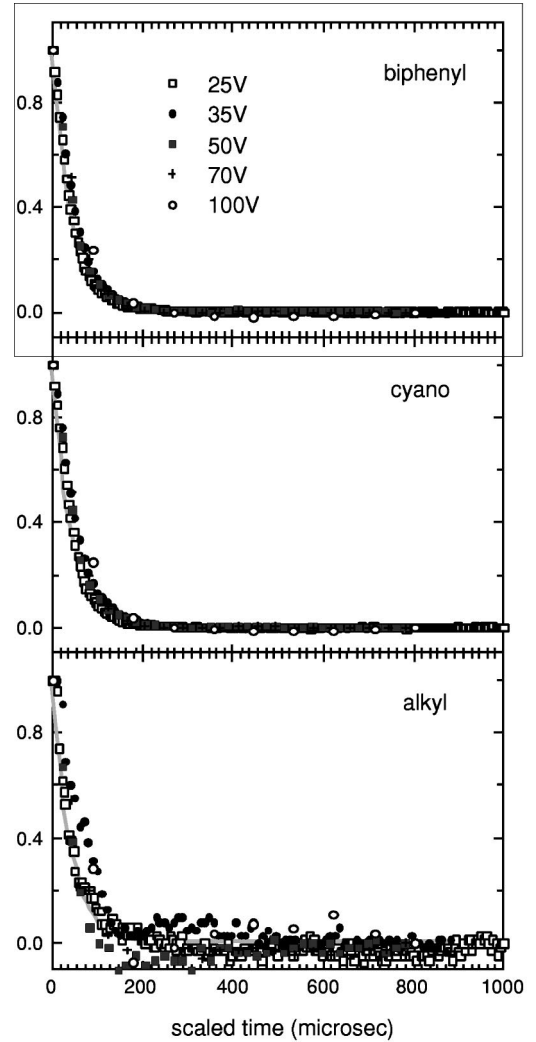


FIG. 5. Normalized absorbance for IR polarization parallel to the plane of reorientation of \mathbf{n} vs scaled time for biphenyl, cyano, and alkyl modes. The time axis for the different voltages is stretched according to $[\text{scaled time} = t_{25V}(V_{\text{pulse}}/25 \text{ V})^2]$. The solid curve is a fit of the $V_{\text{pulse}} = 25 \text{ V}$ data to Eq. (2). The overall response scales as V^{-2} , as expected for the balance of electrical and viscous torques.

the final absorbance in the field-induced homeotropic orientation with $\mathbf{n}(\mathbf{r}) \parallel \mathbf{x}$. If $\mathbf{n}(\mathbf{r})$ is initially uniform and tilted by the angle θ_0 at $t = 0$ then, in response to a voltage step, $\mathbf{n}(\mathbf{r})$ will remain uniform [17] at an angle $\theta(t)$ given by the solution to the equation of motion $d\theta/dt(t) = (\Delta\epsilon E^2/4\gamma)\sin 2\theta(t)$. This solution is $\tan \theta(t) = \tan \theta_0 \exp(\Delta\epsilon E^2/2\gamma)t$, for which

$$\delta A_{\parallel N}\theta(t) = \frac{1 + \tan^2 \theta_0}{1 + \tan^2 \theta_0 \exp(\Delta\epsilon E^2/\gamma)t}. \quad (2)$$

This equation was used to fit the normalized time variation of absorbance.

IV. RESULTS

In a nematic the dichroism ratio $D \equiv A_{\parallel}/A_{\perp}$ is determined for each mode by β , the angle between its absorption dipole and the molecular long axis and by the nematic order parameter S ; The *biphenyl* core and *cyano* stretching vibrations have $\beta \approx 0^\circ$, and thus the largest D ; the *alkyl* CH_2 stretching vibration has $\beta \approx 90^\circ$, for an all-*trans* tail and thus $D < 1$, with D made closer to 1 because of disorder in tails. Figure 3 shows time evolution of A_{\parallel} and A_{\perp} of the three modes for $V_{\text{pulse}} = 25$ V, $\tau_{\text{pulse}} = 1000$ μs . At $t = 0$, $D_{\text{biphenyl}} > 1$, $D_{\text{cyano}} > 1$ and $D_{\text{alkyl}} < 1$, as noted above. With application of the electric field, A_{\perp} is essentially unchanged, as expected for induced reorientation of $\mathbf{n}(\mathbf{r})$ in the \mathbf{x} - \mathbf{z} plane. On the other hand, the induced reorientation of $\mathbf{n}(\mathbf{r})$ in the \mathbf{x} - \mathbf{z} plane decreases $A_{\parallel\text{biphenyl}}$ and $A_{\parallel\text{cyano}}$, while increasing $A_{\parallel\text{alkyl}}$, with $D \rightarrow 1$ for all three modes, indicating that the field induces \mathbf{n} normal to the plates in the bulk of the cell. The $\delta A_{\parallel N}(t)$, measured for the *phenyl*, *cyano*, and *alkyl* peaks at $T = 29^\circ\text{C}$ for $V_{\text{pulse}} = 25, 35, 50, 70$, and 100 V are shown in Fig. 4. Typical times for completion of the reorientation at these voltages are about 150, 80, 40, 18, and 8 μs , respectively, and τ_{pulse} is adjusted so that the pulse ends in about 5 times the switching time in each case. Response times faster than 8 μs were not studied because of the finite RC time constant of the cell.

Because of the pretilt and the finite pulse frequency $\theta(t)$ is nonzero at $t = 0$, and there is torque applied to the director at $t = 0$ so that switching (orientation) commences immediately upon application of the field. These data show no systematic differences among time dependences for absorbance change of the *phenyl*, *cyano*, and *alkyl* peaks, i.e., the observed differences appear to be within the uncertainties due to measurement noise, which is considerably larger for the *alkyl* than for the *phenyl* or *cyano*, because of the small change in A_{\parallel} for the *alkyl*. For field-driven changes of $\mathbf{n}(\mathbf{r})$ of a nematic we expect that t_R , the characteristic time for reorientation of a spatially uniform \mathbf{n} , scale as $t_R \sim \gamma/\Delta\epsilon E^2 \sim E^{-2}$, where γ is the rotational viscosity [18]. The results in Fig. 5 show this scaling behavior for the three vibrations, indicating that reorientation is limited by a frequency independent rotational viscosity down to the fastest time scale studied here $t_R \sim 5$ μs . Some delay in the response may be beginning to appear at the highest voltage, but this is likely a consequence of the finite RC time constant of the cell and the 5 μs step scan time employed. The solid curve in Fig. 5 is a fit of the $V_{\text{pulse}} = 25$ V data to Eq. (2), which yields the ef-

fective initial tilt θ_0 and $t_R \sim \gamma/\Delta\epsilon E^2$. The initial tilt $\theta_0 = 40^\circ \pm 5^\circ$, is governed by pre-tilt and by the relaxation of $n(t)$ to the field-free orientation at the pulse frequency of 1 KHz. t_R is consistent with known 5CB $\Delta\epsilon$ and γ and our estimate of the cell thickness.

V. DISCUSSION

The implementation of the step-scan time-resolved spectroscopy technique allows us to probe the microsecond time-scale reorientation and relaxation dynamics of 5CB cells from planar-to-homeotropic transition. The change in normalized absorbance following application of a voltage step exhibits a universal dependence on scaled time for the core and tail vibrational modes studied. No evidence for differences in the reorientation of different molecular segments was found, except perhaps at the highest voltages and fastest (5 μs) response time observed, where the intrinsic experiment time response is not negligible. Extending these experiments to give time response behavior on time scales 5 μs and faster will require fabrication of IR transparent low capacitance cells [19], experiments which are being planned.

As can be seen from the model, if the internal molecular distortion during switching relaxes at a rate Γ , then the effects of this relaxation become more dramatic as the switching time t_R is driven at a higher field to the regime $t_R < 1/\Gamma$. In the limit $t_R \ll 1/\Gamma$, the dynamic response should become distinctly bimodal, exhibiting a driven reorientation in time t_R to a nonequilibrium state of internal molecular distortion, which would relax on the much longer time scale $1/\Gamma$. The absence of such effects in our data thus implies its absence in slower experiments, and, indeed, no evidence for internal relaxation is found in several slower experiments [2,20,21]. However, our data appear to be fundamentally inconsistent with earlier observations on 5CB and related molecules at much longer time scales, in which such relaxation is found [7,8,13,14]. For example, Urano and Hamaguchi [7] find an apparent delay of about 1 ms in the response of the core relative to that of the tails, which should be quite evident with our setup, but which we do not observe. The origin of such differences is not clear at this time.

ACKNOWLEDGMENTS

This work was supported by NSF MRSEC Grant No. DMR 9809555. The authors are indebted to C. S. Park for stimulating discussions.

-
- [1] A. Kocot, J. kK. Vij, and T. S. Perova, *Adv. Chem. Phys.* **113**, 203 (2000).
 [2] T. Nakano, T. Yokoyama, and H. Toriumi, *Appl. Spectrosc.* **47**, 1354 (1993).
 [3] S. V. Shilov, S. Okretic, and H. W. Siesler, *Vib. Spectrosc.* **9**, 57 (1995).
 [4] N. Katayama, M. A. Czarnecki, M. Satoh, T. Watanabe, and Y. Ozaki, *Appl. Spectrosc.* **51**, 4 (1997).
 [5] S. V. Shilov, H. Skupin, F. Kremer, E. Gebhard, and R. Zentel, *Liq. Cryst.* **22**, 203 (2000).
 [6] S. V. Shilov, H. Skupin, F. Kremer, T. Wittig, and R. Zentel, *Phys. Rev. Lett.* **79**, 1686 (1997).
 [7] T. Urano and H. Hamaguchi, *Chem. Phys. Lett.* **195**, 287 (1992); *Appl. Spectrosc.* **47**, 2108 (1993).
 [8] K. M. Booth, J. Nash, and H. J. Coles, *Meas. Sci. Technol.* **3**, 843 (1992).

- [9] M. A. Czarnecki, N. Katayama, Y. Ozaki, M. Satoh, K. Yoshino, T. Watanabe, and T. Yanagi, *Appl. Spectrosc.* **47**, 1383 (1993).
- [10] H. Toriumi, H. Sugisawa, and H. Watanabe, *Jpn. J. Appl. Phys.* **27**, L935 (1988).
- [11] W. Uhmann, A. Becker, C. Taran, and F. Siebert, *Appl. Spectrosc.* **45**, 390 (1991).
- [12] R. A. Palmer, *Spectroscopy (Amsterdam)* **8**, 26 (1993).
- [13] V. G. Gregoriou, J. L. Chao, H. Toriumi, and R. A. Palmer, *Chem. Phys. Lett.* **179**, 491 (1991).
- [14] K. Huang and G. G. Fuller, *Liq. Cryst.* **25**, 745 (1998); **26**, 1 (1999).
- [15] DEI HV1000, Directed Energy, Inc., Fort Collins, CO, USA.
- [16] Nissan Chemical Co. RN768 polyimide.
- [17] This excludes the penetration layers at the surface of thickness $\xi = \sqrt{K/\Delta\epsilon E^2}$ which at the fields employed here are of negligible thickness.
- [18] P. G. de Gennes and J. Prost, *The Physics of Liquid Crystals*, 2nd ed. (Oxford University Press, Oxford, 1991).
- [19] H. Takanashi, J. E. Maclennan, and N. A. Clark, *Jpn. J. Appl. Phys.* **37**, 2587 (1998).
- [20] H. Sugisawa, H. Toriumi, and H. Watanabe, *Mol. Cryst. Liq. Cryst. Sci. Technol., Sect. A* **214**, 11 (1992).
- [21] J. de Bleijser, L. H. Leyte-Zuiderweg, J. C. Leyte, P. C. M. van Woerkom, and S. J. Picken, *Appl. Spectrosc.* **50**, 167 (1996).